Prediction of the local structure of liquid and supercooled tantalum

N. Jakse,[1,2] O. Le Bacq,[1] and A. Pasturel[1]
[1]*Laboratoire de Physique et Modélisation des Milieux Condensés, Maison des Magistères, BP 166 CNRS, 38042 Grenoble cedex 09, France*
[2]*Laboratoire de Théorie de la Matière Condensée, Université de Metz, 1. bd FD Arago, 57078 Metz Cedex 3, France*
(Received 21 October 2003; revised manuscript received 23 March 2004; published 10 November 2004)

We report first principles molecular dynamics simulations to predict the short-range order of liquid and supercooled tantalum. The results give support to characterize the transitory phase which occurs during solidification from highly undercooled tantalum liquid, as observed in ultravacuum drop tube experiments. The local short range order determined in the supercooled liquid displays a complex polytetrahedral type order, very close to that of the A15 phase. We have also determined the melting temperature of the A15 phase in fine agreement with the experimental melting temperature of the transitory phase, which represents a first step in the understanding of the solidification path.

DOI: 10.1103/PhysRevB.70.174203 PACS number(s): 61.20.Gy, 61.20.Ja

I. INTRODUCTION

Upon supercooling, a liquid becomes metastable with respect to solid state. Under these nonequilibrium conditions, the free energy difference represents a driving force which leads to the formation of various metastable phases. These can be crystalline structures different from those of the stable solid as well as amorphous solids with kinetically arrested liquid-like structure. Investigations of undercooled melts are therefore of great importance not only for a better understanding of fundamental phenomena such as nucleation[1] but also for the subsequent design and engineering of new high-performance materials.

Recently, experimental containerless methods have enabled the observation of a double recalescence phenomenon for Re and Ta metals,[2] giving experimental evidence of an undercooling-induced metastable phase transformation in pure transition metals. Unfortunately, the metastable phases of pure refractory metals induced by the supercooling conditions are transitory during the solidification process, and their melting temperature is the only signature. For Ta, total energy calculations at $T=0$ K coupled with a simple thermodynamic model have been proposed[2,3] to determine the melting temperature of candidate structures. The metastable phase is then determined by comparing the calculated melting temperatures of candidate structures to the experimental melting temperature. For Ta, the A15 phase, which is energetically very close to the bcc crystalline structure, represents a plausible structure for the metastable phase observed in the ultravacuum drop tube experiment.[2,3] However, the proof is quite indirect since it is based on the use of candidate structures chosen intuitively.

Another way would be to study the structure of liquid Ta as a function of temperature above and below the melting point. In this case, the concept is to relate the local structure of the supercooled state to that of the transitory phase. It is based on the similarity of the short-range order (SRO) of liquid and solid phases, which leads to a low solid–liquid interfacial energy and consequently to a low activation threshold for nucleation.[4]

Due to an extremely high melting temperature, the direct experimental observation of the atomic structure of refractory transition metals such as Ta in the liquid state is still out of reach. First-principles based simulations appear then to be crucial to predict their SRO in the liquid and supercooled states. Particularly, *ab initio* MD provides a very accurate tool to study consistently structural, dynamic, and electronic properties of system containing *d*-electron elements.[5,6] The aim of this paper is to elucidate the nature of the SRO of Ta in the liquid state and its evolution in the supercooled region. Using an approach similar to the one used to determine the structural properties of undercooled Zr liquids,[7] we investigate the structural properties of Ta and especially the underlying inherent structures[8] by means of common-neighbor analysis.[9] In this manner, we have access to a detailed three-dimensional image of the local atomic arrangements. It is seen that the fivefold symmetry dominates in the stable liquid and grows upon supercooling. By comparison with the structural and energetic features of the Frank Kasper phases, we show that there is a reinforcement of the A15-type SRO when the liquid is undercooled. We have also determined the melting temperature of the A15 phase and we found a fine agreement with the experimental melting temperature of the transitory phase. Such a study may be considered as a first step towards the understanding of the solidification path.

In Sec. II, we present details of first-principles MD simulations. Section III contains the results and their discussion. A brief summary and conclusions are given in Sec. IV.

II. COMPUTATIONAL DETAILS

We have performed first-principles simulations, using the most recent version of the Vienna *ab initio* simulation package (VASP),[10], based on the density functional theory (DFT) within generalized gradient approximation (GGA).[11] The interaction between the ions and electrons is described by the projector augmented-wave (PAW) method implemented by Kresse and Joubert.[12] In the present PAW potential, the 6*s* and 5*d* orbitals as well as the semi-core 5*p* orbitals are treated as valence orbitals with a plane-wave cutoff of 224 eV (only the Γ point was considered to sample the supercell Brillouin zone).

The phase-space trajectory of the liquid is generated using molecular dynamics in the *NVT* ensemble, by means of a Nosé thermostat to control the temperature, with a time step of 3 fs. Three temperatures were considered, namely $T=3500$ K in the stable liquid well above the experimental melting point of 3287 K and $T=2900$ and 2600 K in the supercooled regime.

At these three temperatures, a cubic cell of volume V containing $N=256$ atoms, subject to standard periodic boundary conditions was used. The size of the simulation box was set to $L=17.24$ Å in order to reproduce the experimental density of liquid tantalum.[13] However, it has been shown[14] that using the density of the liquid state to describe the structural properties of the supercooled state is a rather crude approximation. Therefore, at $T=2600$ K, two other simulations were performed to study the influence of the temperature dependence of the atomic density. The first one has been done with a 216-atom- computational cell with $L=15.93$ Å, which corresponds to a density of the supercooled liquid obtained by assuming a temperature dependence of the atomic density in the supercooled regime similar to that observed above the melting temperature.[13] Let us mention that such an assumption has been very recently confirmed by Paradis *et al.*[15] The second simulation has been done with a 250-atom-computational cell with $L=16.60$ Å, which corresponds to the experimental density of the bcc phase at this temperature. Such a density may be considered as the physical limit of the density of the supercooled state. We have estimated the pressure for this density which is 2.75 GPa. This relatively moderate value represents the upper limit for all the simulations considered here. We mention that the number of atoms have been chosen in order to allow either A15-type long-range order or bcc-type long range order to develop.

The typical duration of the runs is 7.5 ps. The procedure of the simulations is the following: starting at 5000 K from a well equilibrated state, the system is quenched instantaneously at 3500 K at constant volume. This procedure is repeated for other temperatures and other densities. For each run, after an equilibration period of 2 ps, a number of 100 configurations were extracted to produce averaged structural quantities. Among 100 configurations, ten selected configurations regularly spaced in time are saved. The steepest-descent energy-minimization procedure with the conjugate gradient method is imposed on each of these configurations to extract their inherent structures,[8] in which atoms are brought to local minimum in the potential-energy surface.

We have determined the self-diffusion coefficient D from the velocity autocorrelation function, which takes the value $D=0.69\times10^{-4}$ cm^2/s at $T=3500$ K. Upon quenching at constant volume we find $D=0.41\times10^{-4}$ cm^2/s at $T=2900$ K, and $D=0.38\times10^{-4}$ cm^2/s at $T=2600$ K. Then, increasing the density at $T=2600$ K results in an additional lowering of D, namely, $D=0.2\times10^{-4}$ cm^2/s. Nevertheless, the diffusion remains significant even at the lowest temperature and highest density, attesting that the system keeps a liquid-like behavior.

III. RESULTS AND DISCUSSION

A. Pair-correlation functions and bond orientational order

In Fig. 1, we display the pair-correlation function $g(r)$ for all the thermodynamic states as described in the preceding section. Figure 1(a) shows the evolution of $g(r)$ with temperature when the density is kept constant. In quenching the system, it is seen that the first peak narrows and its height increases. This is a characteristic feature accompanying the supercooling, revealing a sharper-defined structure. The peak remains asymmetric, which may be compatible with a bcc-like structure.[7] In Fig. 1(b) the effect of the density is examined at $T=2600$ K, and a shift of the different peaks towards lower distances is seen when the density is increased. This is more visible on the second and third peaks that show a change in their shape as well as a shift of their position towards lower r. This is the first signature that changes occur in SRO in the supercooled regime (as an indication we plot the positions of the atoms in the A15 and bcc structures as solid and dashed vertical bars, respectively).

Taking the first minimum of $g(r)$ as the radius r_c defining the first coordination shell, we find an increase of coordination number from $N_c=13.2\pm0.1$ at $T=3500$ K to $N_c=13.5\pm0.1$ at $T=2600$ K for the density of the supercooled liquid.[13,15] This increase is directly related to the change in density since a coordination number $N_c=13.3\pm0.1$ at $T=2600$ K is obtained when the system is quenched at constant volume.

Figure 2(a) shows the bond-angle distribution $g(\theta)$ at the three temperatures, with the density of the stable liquid. The temperature effect leads to a better defined two-peaks structure. These two peaks are located at $\theta=55°$ and 105°, respectively, and a hump occurs also at $\theta=150°$. The density effect at $T=2600$ K, which is shown in Fig. 2(b), leads to a still more pronounced two-peaks structure and a more defined hump around $\theta=150°$. These results indicate again a change in SRO in the supercooled regime. They can be compared to the angle distribution of the bcc crystal, namely $\theta=55°$, 71°, 90°, 109° and 125° and to that of the more complex distribution of the A15 crystal, namely $\theta=48°$, 57°, 66°, 100°, 114°, and 156°. Let us also mention that the icosahedral symmetry gives angles, namely $\theta=63.5°$ and 116.5° not so far from our results. As these distributions have most of the angles close to each other, it is difficult to distinguish between them in our results.

The preliminary conclusion for liquid Ta is that changes occur in SRO in the supercooled regime. However, if the pair-correlation function $g(r)$ and the bond-angle distribution are adapted to detect the structural evolution, they are not accurate enough to analyze this structural evolution.

B. Pair-analysis technique

In order to obtain a more detailed three-dimensional description of SRO, we resort to the common-neighbor analysis[9] in which the first two peaks of the pair-correlation function are decomposed. This method is able to characterize the local environment surrounding each atomic pair that contributes to the peaks of $g(r)$, in terms of the number and

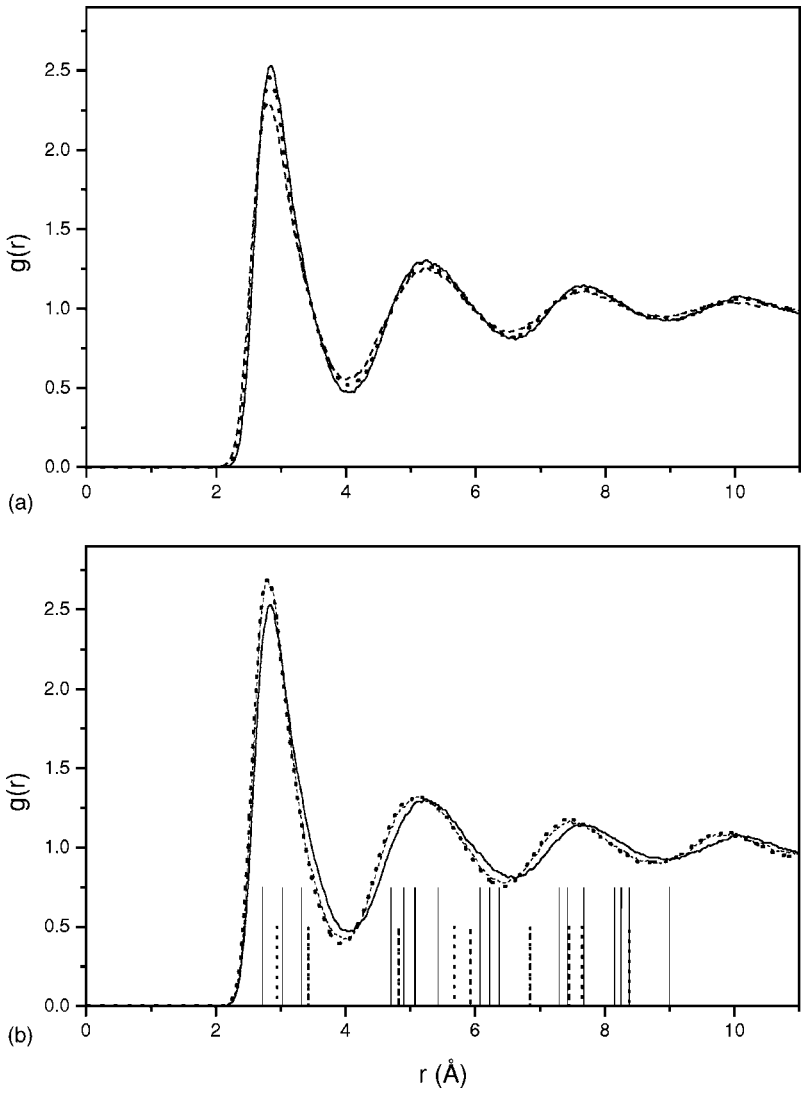

FIG. 1. Pair-correlation function $g(r)$ of Ta: (a) for the quench at constant volume in the liquid at $T=3500$ K (dashed line) and supercooled melts at $T=2900$ K (dotted lines) and 2600 K (solid line); (b) in the supercooled region at $T=2600$ K with a density corresponding to that of the stable liquid (Ref. 13) (solid line), the density of the supercooled liquid (Ref. 13 and 15) (dashed line), and the density of the bcc structure at the considered temperature (dotted line). The solid and dashed vertical bars represent the positions of the atoms for the A15 and bcc lattices, respectively.

properties of common nearest neighbors of the pair under consideration. The positions of the first and second minima are used as a cutoff distance to define the nearest- and second nearest-neighbor atoms, respectively. To avoid the thermal noise, we use the "inherent structure" concept which is a way to resolve observable order in the liquid into the vibrational and inherent structural parts. In the inherent structures, the atoms are brought to local minima of the potential energy surface using a steepest-descent energy-minimization procedure with the conjugate gradient method. For each temperature, ten selected configurations are used to generate the inherent structures. A set of four indices is assigned to each atomic pair contributing to the pair-correlation function: (i) the first index denotes to what peak of $g(r)$ belongs the pair under consideration, i.e., the root pair 1 for the first and 2 for second peak of $g(r)$--; (ii) the second index represents the number of near neighbors shared by the root pair; (iii) the third index is for the number of nearest-neighbor bonds among the shared neighbors; (iv) a fourth index is used to distinguish configurations with the same first three indices but with a different topology. Figure 3 shows the most frequent configurations corresponding to pairs of the first peak.

This method is able to distinguish between various local structures like fcc, hcp, bcc, and icosahedral environments. For example, four bonded pairs are represented in a bulk fcc crystal: 1421, 2101, 2211, and 2441. A bulk hcp contains the same pairs but not with the same weight and additional pairs like 1422 and 2331 pairs. The 1441, 1661, 2101, 2211, and 2441 are typical pairs of the bulk bcc crystal. On the other hand, the 1551 bonded pairs represent the two root pair atoms with five common neighbors that have five bonds, thus forming a pentagon of atoms in contact. Let us emphasize that the number of 1551 bonded pairs is a direct measurement of the degree of icosahedral ordering. For instance, local order built on a 13-atom icosahedron leads to the occurrence of 1551, 1321, and 2331 pairs.

In Table I, we have gathered the relative abundance of the relevant pairs of our simulations at $T=3500$ K and $T=2600$ K (as a function of density) as well as those of the A15 and bcc lattices. The microscopic analysis emerging from the data of Table I indicates that the SRO of the liquid at $T=3500$ K is quite different from the nucleating bcc-type structure since it is dominated by icosahedral and distorted icosahedral inherent structures. Indeed the 1551, 1541, and 1431 bonded pairs are preponderant, the last two pairs (1541

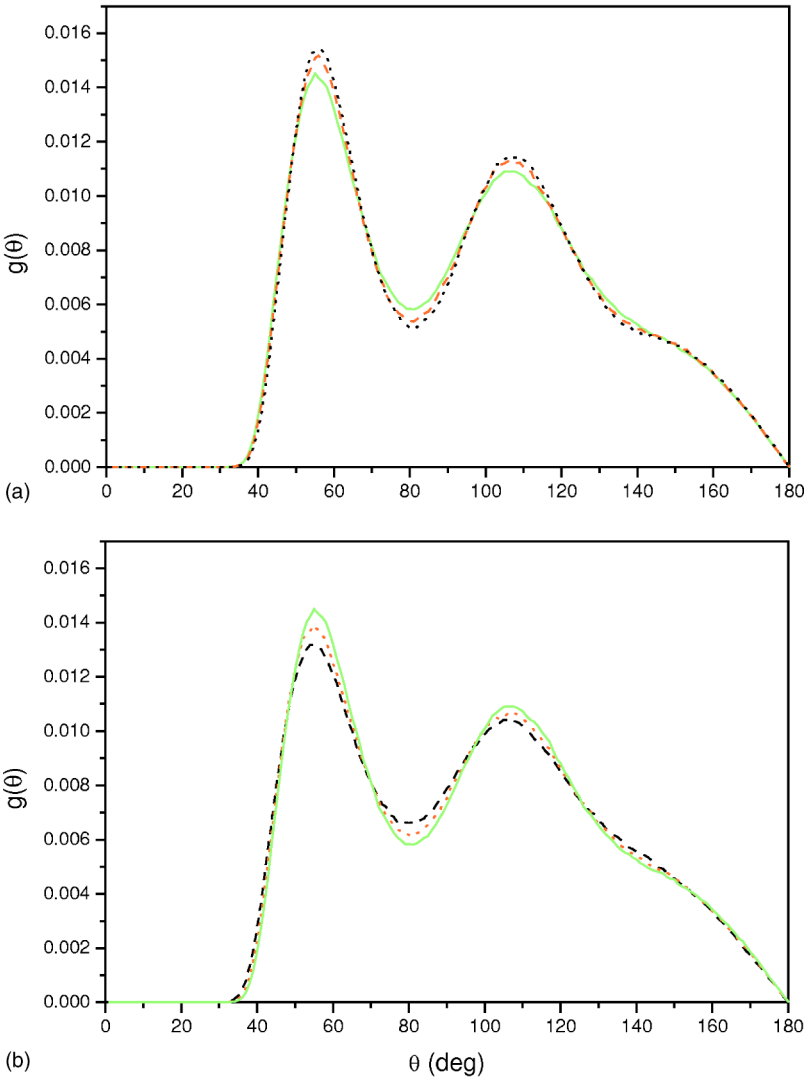

FIG. 2. (Color online) Bond-angle distribution function $g(\theta)$ of Ta (same captions as in Fig. 2).

and 1431) being formed when regular 1551 structures deformed.[15] However, although the 2331 pairs are relatively numerous, the absence of the 1321 pairs and the high value of the 2101 ones is a strong indication that the liquid is characterized by a SRO that is more complex than the one found in the 13-atom icosahedron. The 1441 and 1661 pairs are also of importance. These two pairs may contribute to a bcc-type local structure since the 2101, 2211, and 2441 bonded pairs have a non-negligible weight. However, when associated with the 1551 and 2331 bonded pairs, the 1661 pairs are in favor of Frank–Kasper (FK) polyhedra of high coordination, namely Z14, Z15, and Z16. As already discussed above, the icosahedron is formed by a central atom which has twelve nearest neighbors, all these being joined to it by twelve 1551 bonded pairs. Similarly, if the central atom has fourteen (or more) neighboring atoms, i.e., Z14 (or Z15, Z16), twelve are joined to the central one by twelve 1551 bonded pairs and two (or 3, 4) by two (or 3, 4) 1661 bonded pairs. Therefore, an increasing of the ratio 1661/1551 is a strong indication of an increasing complexity of the Frank–Kasper based-polytetrahedral symmetry.

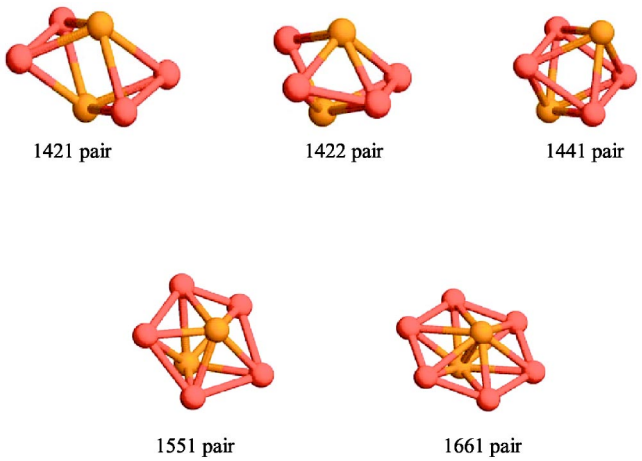

FIG. 3. (Color online) Main atomic pairs of type 1, contributing to the first peak of $g(r)$.

Upon supercooling at constant density, changes are very small and do not show any evolution of SRO. However, taking into account the density introduces noticeable changes. At the density of the supercooled liquid,[13,14] the number of 1551 increases at the expense of the 1431 and 1541 which indicates that defective icosahedra are less nu-

TABLE I. Analysis of the *ab initio* MD simulations in bonded pairs for $T=3500$ K, in the liquid, and $T=2600$ K for the undercooled melt: (a) same density as in the stable liquid, (b) density of the supercooled liquid (Refs. 13 and 15); (c) density corresponding to the bcc structure at the considered temperature, as well as for the bcc and A15 structures. The absolute error bars of the abundances is 0.01.

Bonded pairs	$T=3500$ K	$T=2600$ K[a]	$T=2600$ K[b]	$T=2600$ K[c]	A15	bcc
1551	0.54	0.53	0.55	0.55	0.89	0.00
1541	0.12	0.13	0.10	0.10	0.00	0.00
1431	0.09	0.09	0.07	0.07	0.00	0.00
1421	0.01	0.01	0.00	0.00	0.00	0.00
1422	0.01	0.01	0.00	0.01	0.00	0.00
1201	0.00	0.00	0.00	0.00	0.00	0.00
1211	0.00	0.00	0.00	0.00	0.00	0.00
1301	0.00	0.00	0.00	0.00	0.00	0.00
1311	0.00	0.00	0.00	0.00	0.00	0.00
1321	0.01	0.01	0.00	0.00	0.00	0.00
1331	0.00	0.00	0.00	0.00	0.00	0.00
1441	0.06	0.06	0.08	0.08	0.00	0.57
1661	0.13	0.14	0.16	0.17	0.11	0.43
1771	0.00	0.00	0.00	0.00	0.00	0.00
1881	0.00	0.00	0.00	0.00	0.00	0.00
2101	1.57	1.59	1.59	1.56	1.67	1.57
2211	0.75	0.74	0.73	0.75	0.33	1.71
2321	0.03	0.03	0.01	0.01	0.00	0.00
2331	1.21	1.20	1.21	1.20	1.70	0.00
2441	0.17	0.18	0.20	0.21	0.00	0.86

merous in the supercooled state. However, the competition between fivefold symmetry and the bcc-type symmetries is reinforced since the number of 1551 (with 1541 and 1431) bonded pairs decreases while the number of 1441 and 1661 pairs increases. Thus these two simultaneous variations support the occurrence of a more pronounced bcc-type structure as well as an increasing complexity of the Frank–Kasper based-polytetrahedral symmetry in the supercooled regime. Such a trend is confirmed by the results obtained using a density which corresponds to that of the bcc structure at $T=2600$ K (see column 5 of Table I). In this case, the bcc-type SRO becomes more pronounced. In addition, the evolution of the unbounded pairs shows a simultaneous increase of the 2441 and 2211, which is in favor of a growing degree of the bcc-type ordering.

Among the Frank–Kasper phases, the A15 phase is known to present the smallest percentage of icosahedral sites[3] and consequently the most important polytetrahedral SRO. As already discussed above, the ratio 1661/1551 can be used to discuss quantitatively the degree of the Frank–Kasper based-polytetrahedral symmetry. This ratio can be calculated in the liquid and supercooled states by subtracting the bcc-type contribution from the 1661 pairs. The calculated ratio varies from 0.115 in the liquid state to 0.131 in the supercooled state while it is equal to 0.125 in the A15 phase. Then, we can see that the effect of supercooling via the density variation is to give a polytetrahedral SRO with a symmetry which is very close to that found in the A15 structure.

C. Melting temperature of the A15 phase

In addition to the structure of the supercooled liquid, we have also explored Ta solidification since it is experimentally known that the solidification path of the highly undercooled Ta liquid involves a transitory metastable phase.[2] Our simulations in this regard were done at a constant volume from a supercooled Ta liquid obtained at $T=2600$ K. The simulations have been done with the 250-atom computational cell and with the 216-atom cell which allow the occurrence of long-range orders of bcc-type and A15-type, respectively. For the first cell, the calculated bcc volume has been chosen while for the second cell, the calculated A15 volume has been used (see Fig. 4). At both volumes, thermal quenches lead to a glass structure which displays local characteristics similar to both the bcc and A15 phases. Even if these simulations are unable to reproduce a recrystallization path due to the smallness of the simulation cells,[16] they clearly demonstrate the close competition between the two phases. Such a result can be related to the small energy difference between the two phases at $T=0$ K (see Fig. 4). Indeed, such calculations at $T=0$ K can be used to evaluate the melting temperature of the metastable A15 phase and provides a first indication of the solidification path.

In this work, we use a more elaborate method than that of Ref. 2. The melting temperature T_m of an element can be calculated from the knowledge of its Helmholtz free energy,[17];

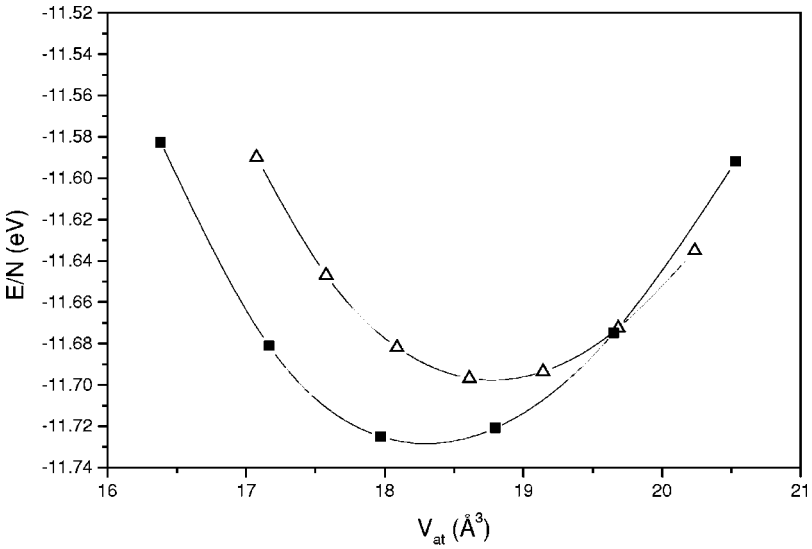

FIG. 4. Structural energies as a function of atomic volume for the bcc and A15 structures. The energy for the supercooled liquid found in the simulation at 2600 K is −10.33 eV at an atomic volume of 18.97 Å^3.

$$T_m = CR^2 \frac{\partial^2 F(V,T_m)}{\partial R^2},$$

where C is a constant for a given element and R is the Wigner–Seitz radius of the atom. The Helmhotz free energy $F(V,T)$ can be written as a sum of three contributions, the total energy at $T=0$ K, the vibrational free energy of the lattice and the free energy due to the thermal excitation of electrons. When the magnetic and the electron–phonon interactions are neglected, the last term is obtained from the knowledge of the electronic density of states.[18] To calculate the vibrational free energy of the lattice, we use the Debye–Grüneisen theory in which the Debye temperature is related to the calculated bulk modulus.[19] Therefore, the only parameter to calculate the melting temperature is the constant C which is simply determined from a fit to the experimental melting temperature of bcc Ta, i.e., 3287 K. Keeping this value of C for the metastable A15 phase leads to a melting temperature of this phase equals to 2910 K, in fine agreement with the measured temperature of 2930±10 K, given in Ref. 2.

IV. CONCLUSION

In summary, we have investigated the SRO of liquid Ta and its evolution upon supercooling by *ab initio* MD simulation. The identification of inherent structures obtained by the common-neighbor analysis indicates that the SRO is dominated by structural units with the fivefold symmetry in the stable liquid which strengthen upon supercooling. Such a result gives an unambiguous proof that the SRO of liquid Ta is independent of the nucleating bcc solid phase. In the undercooled state, the classification of inherent structures clearly points out a polytetrahedral SRO very close to that found in the A15 structure as well as a reinforcement of the bcc-type SRO. This competition gives strong support to the scenario in which supercooling of Ta is accompanied by the formation of a metastable A15 phase as observed in the recent experiments by a double recalescence phenomenon.[2] We calculate the melting temperature of the metastable A15 phase which can be considered as the first step in the understanding of the solidification path.

ACKNOWLEDGMENT

The authors acknowledge PHYNUM-CIMENT-UJF at LPMMC for computational resources on the PC cluster.

[1] D. R. Nelson and F. Spaepen, Solid State Phys. **42**, 1 (1989).
[2] L. Cortella, B. Vinet, P. Desre, A. Pasturel, A. T. Paxton, and M. van Schilfgaarde, Phys. Rev. Lett. **70**, 1469 (1993).
[3] C. Berne, A. Pasturel, M. Sluiter, and B. Vinet, Phys. Rev. Lett. **83**, 1621 (1999).
[4] D. Holland-Moritz, Int. J. of Non-Equilib. Proces. 11, 169 (1999).
[5] G. Kresse and J. Hafner, Phys. Rev. B **48**, 13 115 (1992).
[6] A. Pasquarello, K. Laasonen, R. Car, C. Lee, D. Vanderbilt, Phys. Rev. Lett. **69** 1982 (1992).
[7] N. Jakse and A. Pasturel, Phys. Rev. Lett. **91**, 195501 (2003).
[8] F. H. Stillinger and T. A. Weber, Phys. Rev. A **25**, 978 (1982).
[9] J. D. Honeycutt and H. C. Andersen, J. Phys. Chem. **91**, 4950 (1987).
[10] G. Kresse and J. Furthmüller, Comput. Mater. Sci. **6**, 15 (1996), Phys. Rev. B **54**, 11 169 (1996).
[11] Y. Wang and J. P. Perdew, Phys. Rev. B **44**, 13 298 (1991).
[12] G. Kresse and D. Joubert, Phys. Rev. B **59**, 1758 (1999).
[13] B. Vinet, J. P. Garandet, and L. Cortella, J. Appl. Phys. **73**, 3830 (1993), and references therein.
[14] N. Jakse and A. Pasturel, J. Chem. Phys. **120**, 6124 (2004).
[15] P.-F. Paradis, T. Ishikawa, and S. Yoda, Appl. Phys. Lett. **83**, 4047 (2003).
[16] J. A. Moriarty, J. F. Belak, R. E. Rudd, P. Soderlind, F. H. Streitz, and F. H. Yang, J. Phys.: Condens. Matter **14**, 2825 (1999).
[17] Y. Wang, R. Ahuja, and B. Johansson, Phys. Rev. B **65**, 014104 (2001).
[18] T. Jarlborg, E. G. Moroni, and G. Grimvall, Phys. Rev. B **55**, 1288 (1997).
[19] V. I. Moruzzi, J. F. Janak, and K. Schwarz, Phys. Rev. B **37**, 790 (1988).